Supporting Information for

Structures of the inhibitory receptor Siglec-8 in complex with a high affinity sialoside analog and therapeutic antibody.

Maria Pia Lenza[1], Unai Atxabal[1], Corwin Nycholat[2], Iker Oyenarte[1], Antonio Franconetti[1], Jon Imanol Quintana[1], Sandra Delgado[1], Reyes Núñez-Franco[1], Carmen Teresa Garnica Marroquín[3], Helena Coelho[4], Luca Unione[1], Gonzalo Jiménez-Oses[1, 5], Filipa Marcelo[4], Mario Schubert[6], James C. Paulson[2], Jesús Jiménez-Barbero,[1,3,5,7*] and June Ereño-Orbea[1,5*]

[1] CIC bioGUNE, Bizkaia Technology Park, Building 800, Derio-Bizkaia 48160, Spain

[2] Department of Molecular Medicine and Department of Immunology and Microbiology, The Scripps Research Institute, La Jolla, California 92037, United States

[3] Department of Organic Chemistry II, Faculty of Science and Technology, University of the Basque Country, Leioa 48940, Spain

[4] UCIBIO, REQUIMTE, Departamento de Química, Faculdade de Ciências e Tecnologia, Universi-dade de Nova de Lisboa, Caparica 2829-516, Portugal

[5] IKERBASQUE, Basque Foundation for Science and Technology, Euskadi Plaza 5, Bilbao 48009, Spain

[6] Department of Biosciences, University of Salzburg, Hellbrunnel Str. 34, Salzburg 5020, Austria

[7] Centro de Investigacion Biomedica En Red de Enfermedades Respiratorias, Madrid 28029, Spain.

* Jesús Jiménez Barbero, and June Ereño-Orbea
Email: jjbarbero@cicbiogune.es; jereno@cicbiogune.es

This PDF file includes:

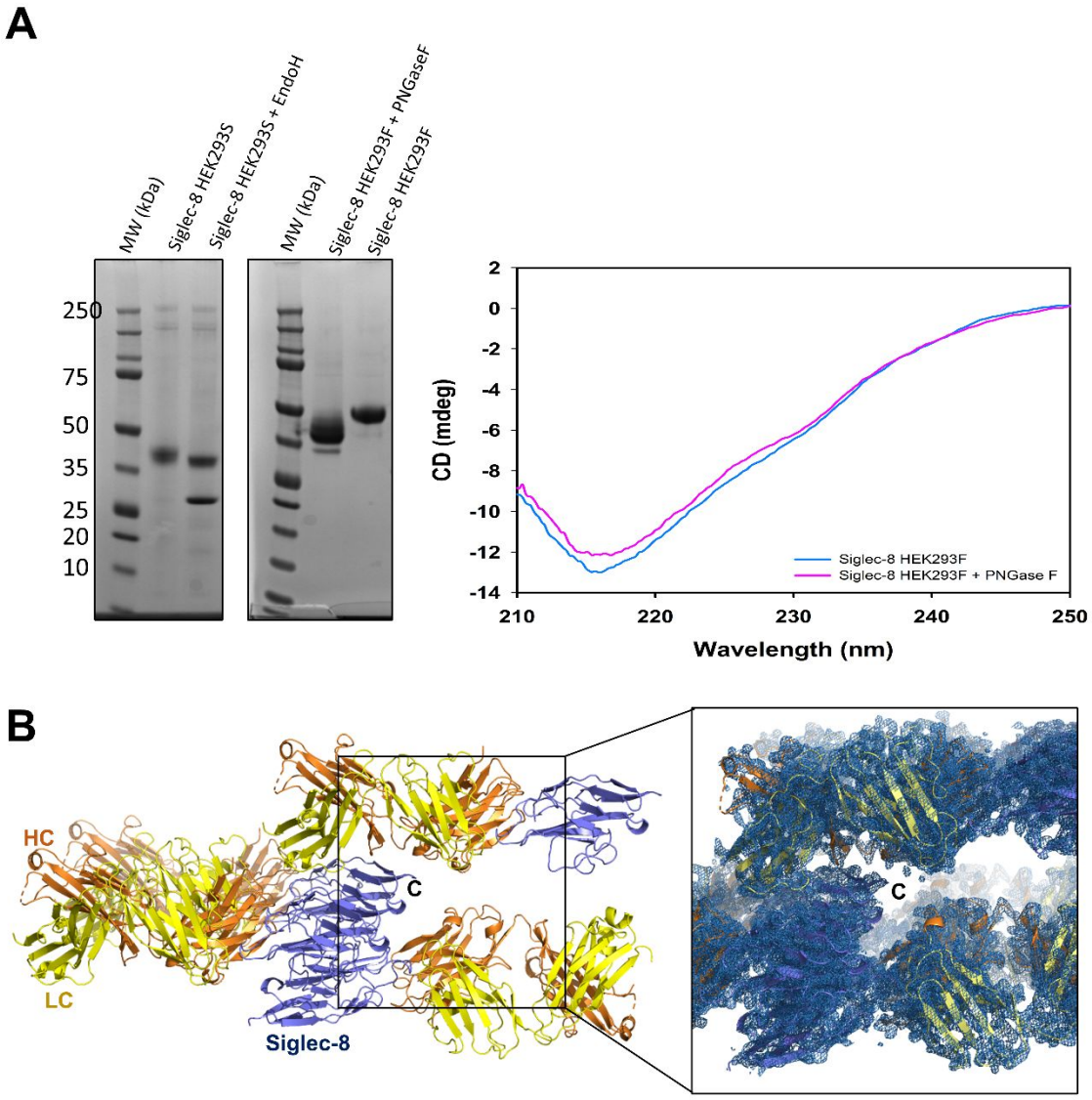

Fig. S1. Crystallization of the glycosylated extracellular domain of Siglec-8. A) Left, SDS-PAGE gel showing the bands corresponding to the purified Siglec-8_{d1d3} protein expressed in HEK293F cells (with complex N-linked glycans) before and after treatment with PNGase F, and expressed in HEK293S (with high-mannose N-glycans) before and after treatment with EndoH. Right, circular dichroism spectra for Siglec-8_{d1d3} expressed in HEK293F before and after PNGase treatment. B) Crystal packing of Siglec-8-2C4 Fab crystal. The Siglec-8 is represented in blue, while the 2C4 Fab is colored in orange (heavy chain) and yellow (light chain). Composite omit map contoured at 1σ is shown with a blue mesh.

A

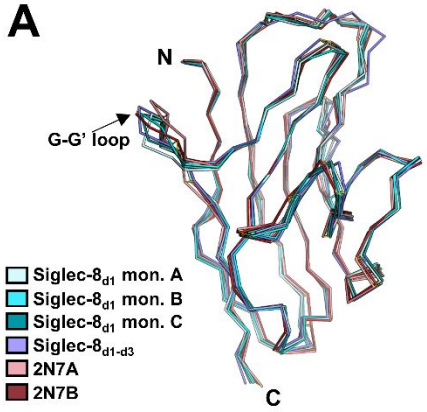

B

	Siglec-8_{d1} mon. A	Siglec-8_{d1} mon. B	Siglec-8_{d1} mon. C	Siglec-8_{d1-d3}	2N7A	2N7B
Siglec-8_{d1} mon. A	-	0.33	0.36	0.51	0.76	0.75
Siglec-8_{d1} mon. B	0.33	-	0.35	0.46	0.78	0.77
Siglec-8_{d1} mon. C	0.36	0.35	-	0.46	0.75	0.76
Siglec-8_{d1-d3}	0.51	0.46	0.46	-	0.84	0.83
2N7A	0.74	0.78	0.75	0.80	-	0.52
2N7B	0.74	0.77	0.75	0.80	0.52	-

Fig. S2. Structural comparison of Siglec-8 V-type Ig domains solved by X-ray crystallography and NMR. A) Superposition of Siglec-8 V domain crystal structures (represented in ribbon) with the NMR structures (PDB IDs 2N7A and 2N7B). B) Cα r.m.s.d. values calculated with Pymol (1) from the superposition of Siglec-8 V domains solved from crystal structures and the NMR structures (PDB IDs 2N7A and 2N7B).

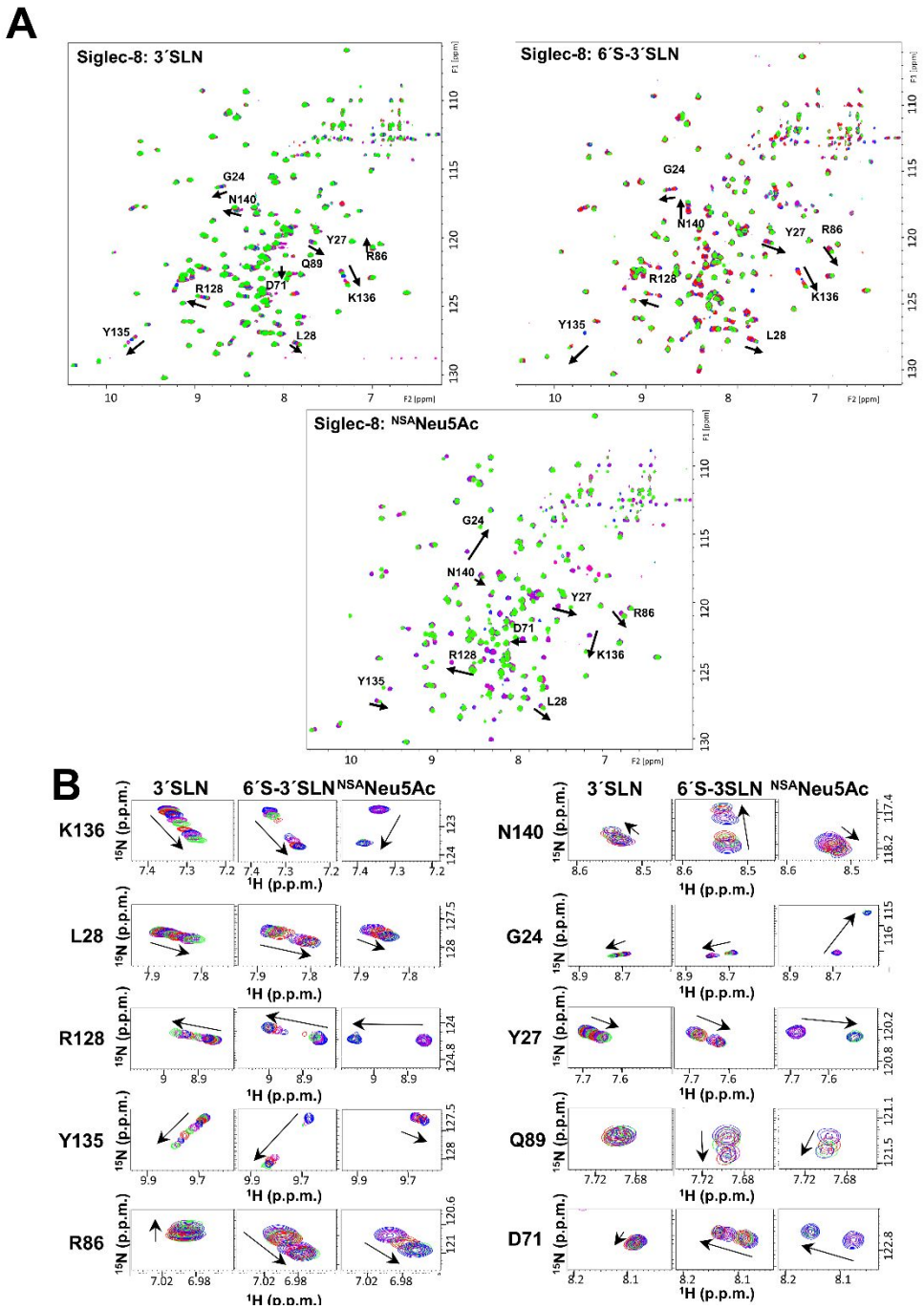

Fig. S3. ^{1}H-^{15}N TROSY HSQC experiments to study the interaction of Siglec-8 with 3´SLN, 6´S-3´SLN and ^{NSA}Neu5Ac. A) Superimposition of ^{1}H-^{15}N-TROSY spectra of the V-domain of Siglec-8 with increasing amounts of ligand. In all the experiments, protein was completely saturated with different concentrations of the ligand. B) Comparison of the most perturbed peaks during the titration with each ligand. Most of the peaks move in the same direction suggesting a similar binding mode. The glycomimetic ^{NSA}Neu5Ac shows big CSPs. Some peaks disappear after the addition of 0.5 equivalents of ^{NSA}Neu5Ac.

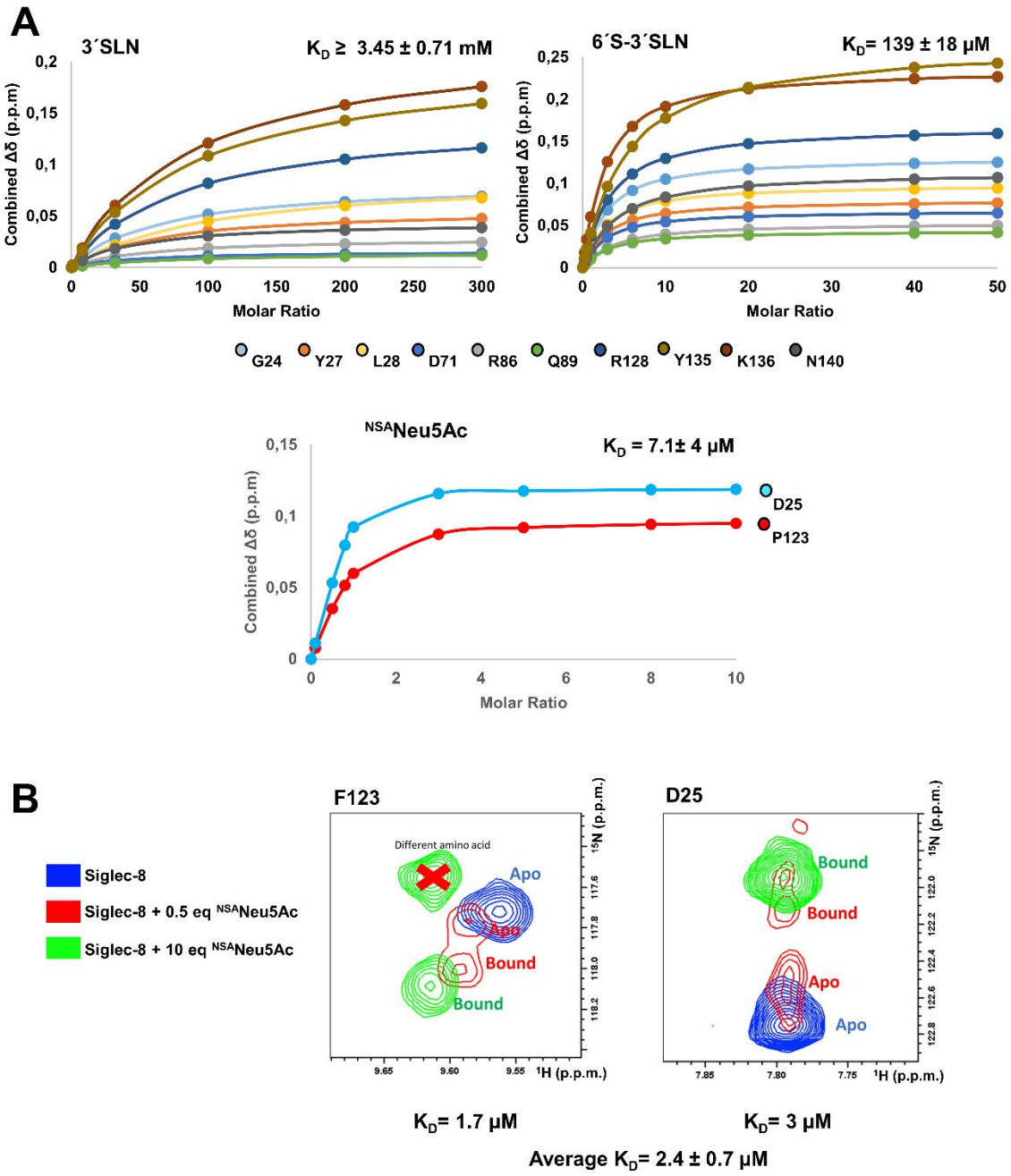

Fig. S4. Determination of dissociation constants (K_D) for binding of Siglec-8 and 3´SLN, 6´S-3´SLN and ^{NSA}Neu5Ac. A) K_D values determined by fitting the combined $^{1}H/^{15}N$ chemical shift changes ($\Delta\delta$) of ^{15}N-labeled Siglec-8 observed in 2D $^{1}H,^{15}N$-HSQC spectra upon titration with each ligand, as described in Materials and Methods. B) ^{1}H-^{15}N-TROSY spectra of F123 and D25 amino acid residues of Siglec-8 in the presence of different ^{NSA}Neu5Ac equivalents. At 0.5 equivalents, both apo and bound forms are observed simultaneously; while at 10 equivalents, a small shift is observed. This is an indication of slow-intermediate regime. K_D values obtained by following shift changes and integrating the peak volumes are indicated.

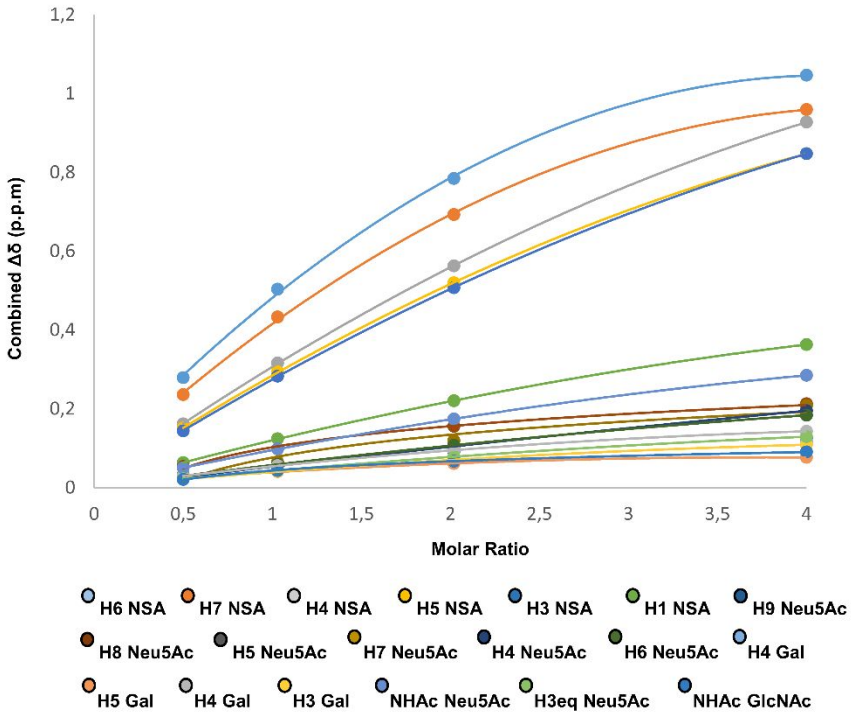

Fig. S5. STD build-up curve for ^{NSA}Neu5Ac. The intensities of STD signals obtained at different saturation times (0.5 s, 1 s, 2 s and 4 s) are plotted and fitted following the mono-exponential equation to obtain normalized STD signals, as explained in *Materials and Methods.*

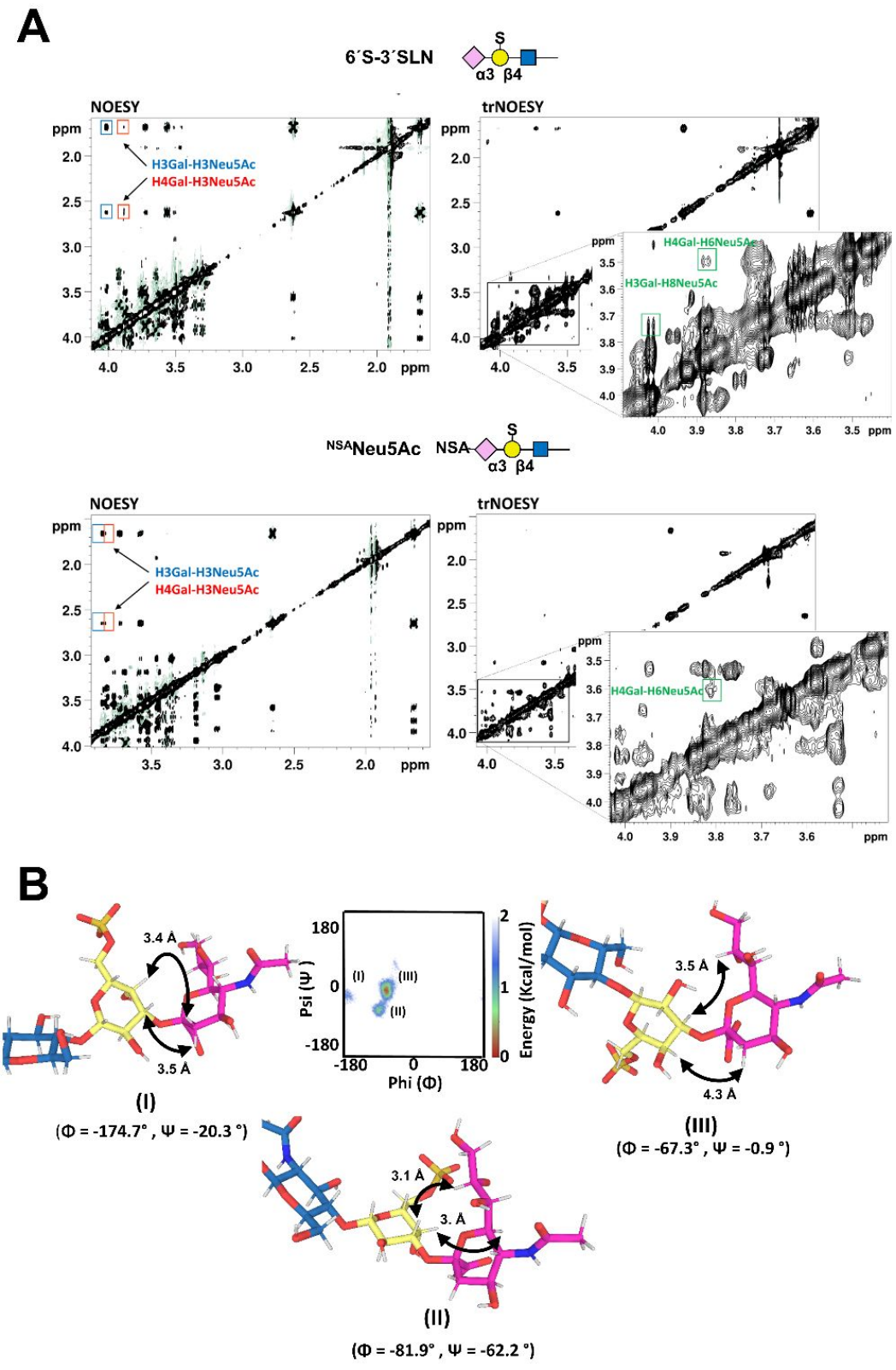

Fig. S6. Conformational analysis of ligands 6´S-3´SLN and ^{NSA}Neu5Ac. A) Comparative 2D ^{1}H-NMR NOESY spectra of 6´S-3´SLN and ^{NSA}Neu5Ac free in solution (NOESY) and in complex with Siglec-8_{d1} (trNOESY). Some

significant cross-peaks that served to determine the conformation of the ligands are highlighted. In red the NOE between H4Gal and H3Neu5Ac and in blue the NOE between H3Gal and H3Neu5Ac are represented. In green, the key NOEs represent the bound conformation. In the presence of Siglec-8 cross peaks between H3Gal - H3eq/ax Neu5Ac (blue), and H4Gal – H3eq/ax Neu5Ac (red) vanish, indicating a conformational selection. In green, some key cross peaks, which give hints of the bioactive conformation. B) Conformational analysis of the glycan core, calculated with AMBER (glycam_06j-1, 500 ns). The Φ/Ψ dihedrals angles in the Neu5Ac(α2,3)-6´-O-sulfo-Gal are plotted showing the presence of 3 different (I, II and III) main populations in solution. The dihedral angles are defined in the following way (Φ: $C1_{Neu5Ac}$ - $C2_{Neu5AC}$ - $O_{glycosidic}$ - $C3_{Gal6S}$ / Ψ: $C2_{Neu5AC}$ - $O_{glycosidic}$ - $C3_{Gal6S}$ - $H3_{Gal6S}$).

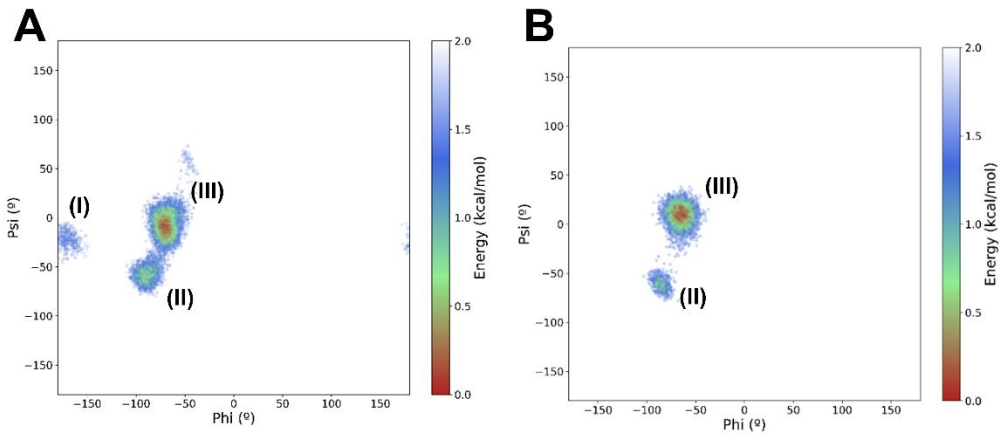

C

Proton Pair	(I) ϕ/ψ -170º/-20º	(II/III) ϕ/ψ 74 ± 7º/-30 ±30º	Experimental Intensity NOESY	Experimental Intensity trNOESY
H3eq Neu5Ac-H3Gal	3.4	4.4 ± 0.2	weak	not observed
H3ax Neu5Ac-H3Gal	2.1	4.0 ± 0.2	medium	very weak
H3eq Neu5Ac-H4Gal	4.7	4.7 ± 0.3	very weak	not observed
H3ax Neu5Ac-H4Gal	3.5	4.9 ± 0.2	medium-weak	not observed
H8 Neu5Ac-H3Gal	4.5	3.3 ± 0.3	medium	medium
H6 Neu5Ac-H4Gal	4.7	4.5 ± 0.7	weak	medium-weak

Fig. S7. Conformations adopted by 6´S-3´SLN in free and bound states calculated with MD simulations. A) Conformation of 6´S-3´SLN in solution. B) Conformation of 6´S-3´SLN in complex with Siglec-8_{d1}. C) Table of the interproton distances estimated for the different energy minimum conformations around the Neu5Acα2,3Gal glycosidic linkage, predicted by the MD simulations. The distances for conformers II and III are given together in the same column, since they can also be considered as belonging to a wide energy minimum region. The experimental intensities observed for 6´S-3´SLN in the free state (NOESY) and when bound to Siglec-8 (trNOESY) are also given. The observed NOEs for the free sate are in agreement with a conformational equilibrium among the 3 different conformers. In contrast, those for the bound state match with a conformational selection process towards the region defined by conformers II/III (Φ 74±7º).

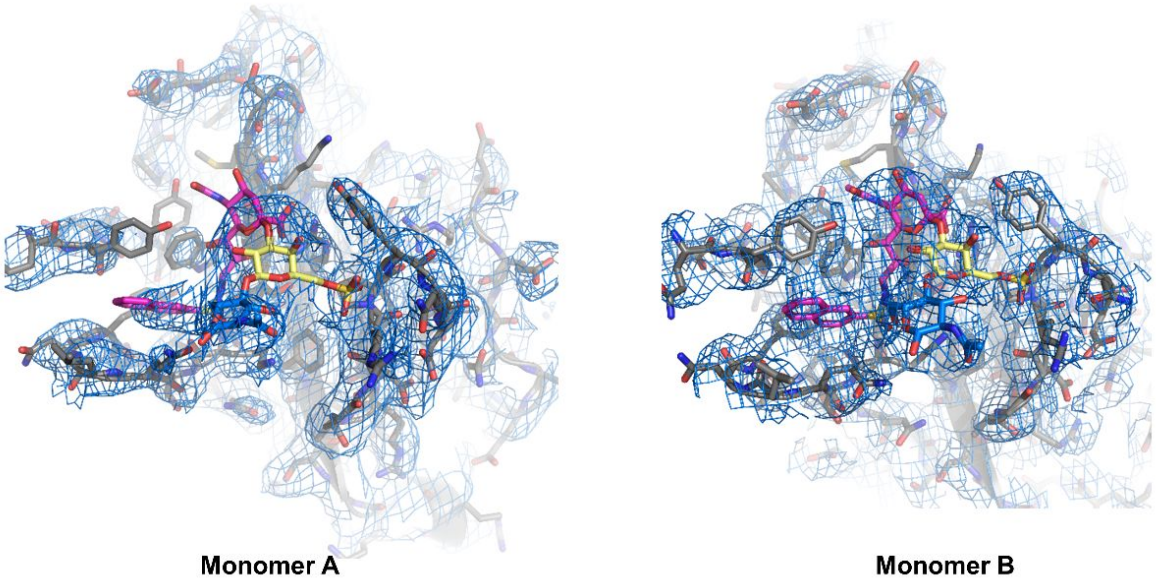

Fig. S8. Representative electron density for Siglec-8 molecules A and B in complex with ^{NSA}Neu5Ac in the crystal structure. Composite omit map was contoured at 1σ and depicted with a blue mesh.

A

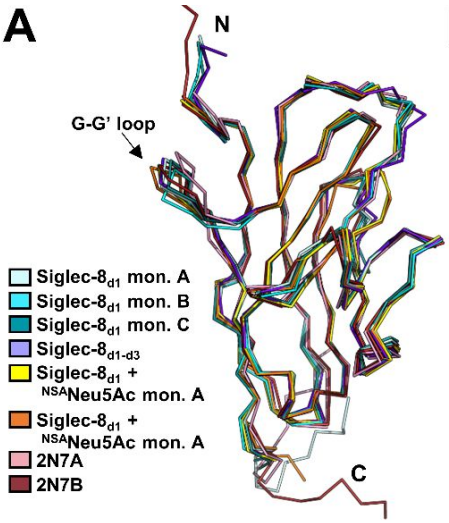

B

	Siglec-8_{d1} + ^{NSA}Neu5Ac mon. A	Siglec-8_{d1} + ^{NSA}Neu5Ac mon. A
Siglec-8_{d1} + ^{NSA}Neu5Ac mon. A	-	0.37
Siglec-8_{d1} + ^{NSA}Neu5Ac mon. B	0.38	-
Siglec-8_{d1} mon. A	0.43	0.38
Siglec-8_{d1} mon. B	0.46	0.44
Siglec-8_{d1} mon. C	0.46	0.43
Siglec-8_{d1-d3}	0.46	0.43
2N7A	0.95	0.82
2N7B	0.88	0.81

Fig S9. Structural comparison of the crystal structure of Siglec-8 bound to ^{NSA}Neu5Ac with other Siglec-8 V-type Ig domains solved by X-ray crystallography and NMR. A) Superposition of Siglec-8 V domain crystal structures (represented in ribbon) with the NMR structures (PDB IDs 2N7A and 2N7B). B) Cα r.m.s.d. values calculated with Pymol (1) from the superposition of Siglec-8 V domains (residues 22-153).

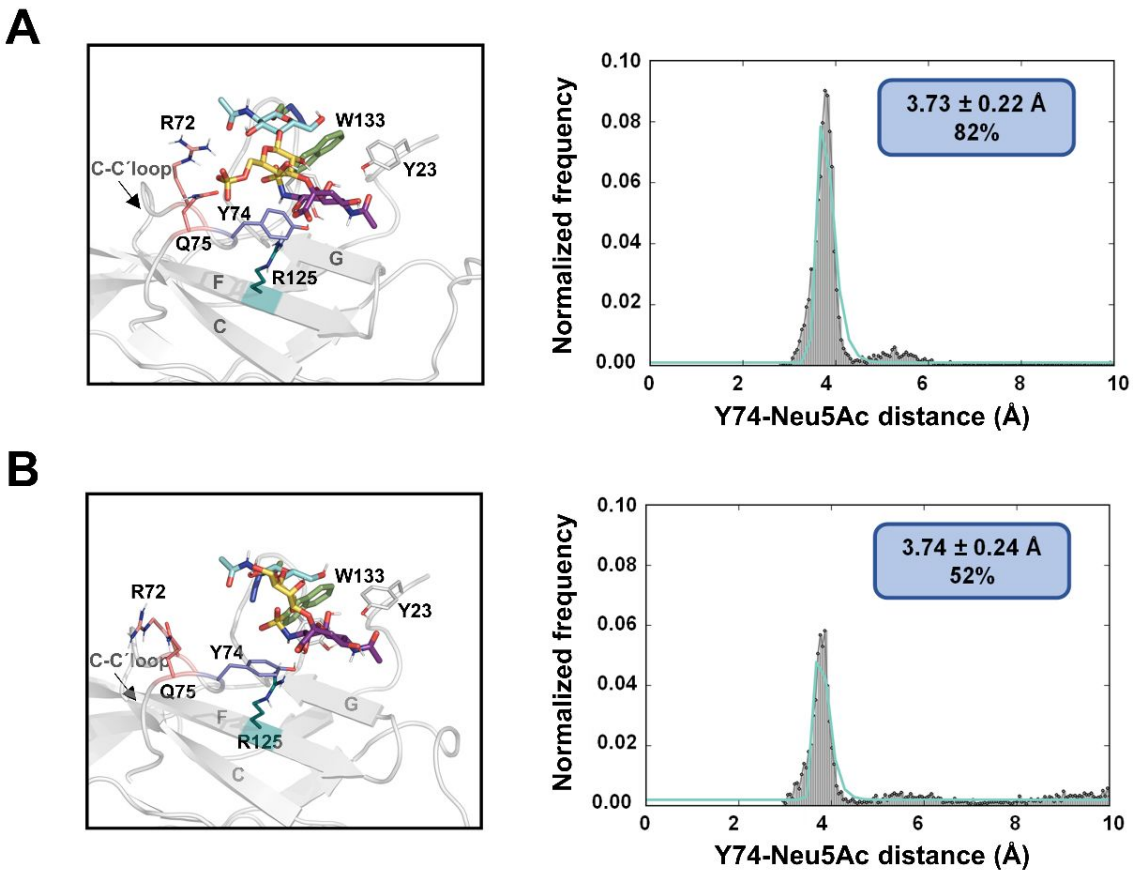

Fig. S10. Structural analysis of the interaction between Siglec-8 and ^{NSA}Neu5Ac analyzed by molecular dynamics simulation. A) (Left) Most frequent conformer of Y74 (in blue sticks) found in the MD simulations of Siglec-8 (in cartoon) bound to ^{NSA}Neu5Ac (in sticks; with NSA in green, Neu5Ac in pink, sulfated Gal in yellow and GlcNAc in cyan). (Right) Histogram showing the distances calculated between the oxygen of the hydroxyl group of Y74 and the carboxylate carbon of Neu5Ac. Average and SD value is depicted inside the blue box. B) Alternative conformation of Y74 (blue sticks). The blue box contains the average and standard deviation for the distance measured when the Y74 hydrogen bonds the Neu5Ac.

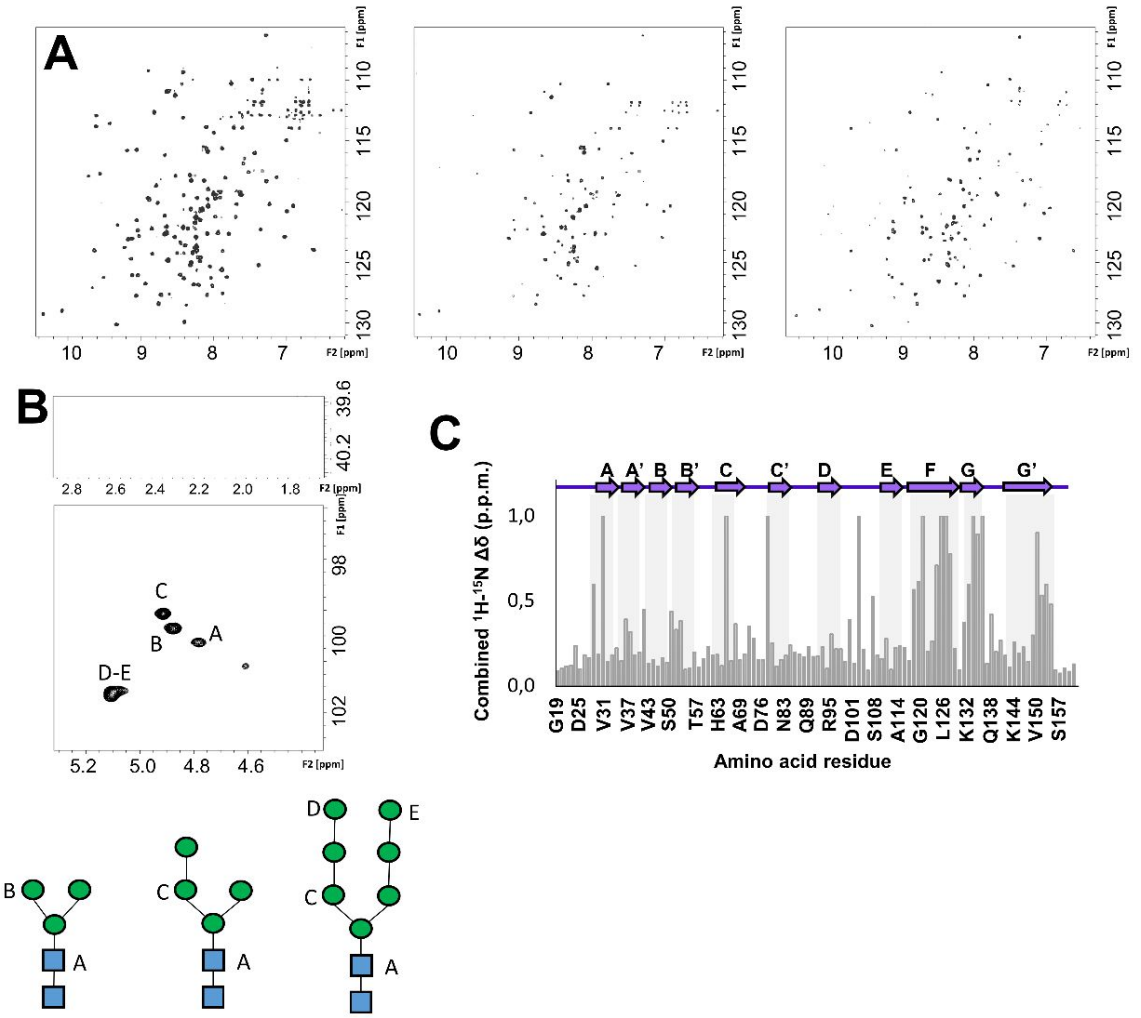

Fig. S11. Interaction of Siglec-8 with N-linked glycans present on the surface of human FcεRIα glycoprotein. A) Competition assay between and ^{NSA}Neu5Ac. (Left) ^{1}H-^{15}N-TROSY spectra of Siglec-8_{d1} in the apo form. (Middle) ^{1}H-^{15}N-TROSY spectra of Siglec-8_{d1} in complex with 1 equivalent of FcεRIα. (Right) ^{1}H-^{15}N-TROSY spectra of the Siglec-8_{d1}-FcεRIα complex with 10 equivalents of ^{NSA}Neu5Ac. B) Details of the anomeric region and of the region containing the axial and equatorial H3 protons of the Neu5Ac residues of the FcεRIα expressed in HEK293S cells showing the presence of only mannose residue. C) Combined ^{1}H–^{15}N chemical shift changes (Δδ) of the ^{15}N-labeled Siglec-8_{d1} observed upon NMR titration with 1 equivalent of FcεRIα expressed in HEK293F cells. The β-strands derived from the crystal structure of Siglec-8_{d1} are represented at the top with blue arrows.

Tables

Table S1. Residues involved in the Siglec-8 and 2C4 Fab interaction. S= salt bridge; H= hydrogen bond.

Contact type	Siglec-8 residue	BSA (Å²)
	G19	18
	D20	41
H	R21	76
H	D25	31
	G26	11
	F49	2
	S50	22
H	Y51	35
	P52	28
H	Q53	162
H	D54	36
	G55	29
	W56	64
	T57	63
HS	D58	120
H	S59	40
	W103	23
H	N105	30
	R128	2
	S130	19
	Total	**852**
	2C4 HC residue	**BSA (Å²)**
H	T30	49
H	I32	50
	Y33	1
H	G34	12
	W55	78
H	A56	30
H	G57	45
	G58	4
H	S59	17
	N61	7
	D76	5
	N77	46
	S78	6

H	D100	12
H	S100C	6
H	P100D	74
	Y101	1
H	Y102	78
	S104	4
	Total	**525**
	2C4 LC residue	**BSA (Å²)**
	S32	24
	Y33	53
HS	H35	9
H	R103	51
H	S104	40
	S105	4
	Y106	34
	F108	14
	Total	**229**

Table S2. Epitope residues of 3´SLN calculated from STD experiments with 1:50 equivalents of ligand in the presence of Siglec-$8_{d1\text{-}d3}$.

	STD-AF	STD epitopes (%)
H9R Neu5Ac	0.76	22.7
H9S Neu5Ac	2.14	64.1
H8 Neu5Ac	1.14	34.2
H5 Neu5Ac	0.93	27.8
H6 Neu5Ac	2.15	64.4
H4 Neu5Ac	2.04	61.3
H7 Neu5Ac	1.69	50.6
NAc Neu5Ac	3.33	100
H5 Gal	0.43	12.9
H6 Gal	0.43	12.9
H3 Gal	0.46	13.8
H4 Gal	0.62	18.6
H3eq Neu5Ac	0.64	19.1
H3ax Neu5Ac	0.64	19.1

Table S3. Epitope residues of 6´S-3´SLN calculated from STD experiments with 1:50 equivalents of ligand in the presence of Siglec-8_{d1}.

	STD-AF	STD epitopes (%)
H9R Neu5Ac	0.12	52.2
H9S Neu5Ac	0.21	89.1
H8 Neu5Ac	0.12	52.2
H5 Neu5Ac	0.12	52.2
H6 Neu5Ac	0.19	80.4
H4 Neu5Ac	0.19	80.4
H7 Neu5Ac	0.21	89.1
NAc Neu5Ac	0.23	100
H5 Gal	0.06	26.1
H6 Gal	0.06	26.1
H4 Gal	0.05	21.7

Table S4. Epitope residues of ^{NSA}Neu5Ac calculated from STD experiments with 1:40 equivalents of ligand in the presence of Siglec-8_{d1}. Since the signals of the glycan scaffold were very low compared with the aromatic signals, STD percentages were also calculated considering only most intense signal of H9R in Neu5Ac.

	STD_{max}	K_{sat}	STD(fit)	STD epitopes (%)	Relative STD epitopes (%)
H6 Napht	118.423	0.53801	0.63712	100	
H7 Napht	113.494	0.46688	0.52988	83.2	
H4 Napht	164.758	0.20699	0.34103	53.5	
H5 Napht	144.502	0.22081	0.31907	50.1	
H3 Napht	15.889	0.19057	0.30279	47.5	
H1 Napht	0.64409	0.20768	0.13376	21.0	
H8 Napht	0.14995	0.47091	0.07061	11.1	
H9S Neu5Ac	0.2477	0.49128	0.12169	19.1	100
H5 Neu5Ac	0.42439	0.14238	0.06042	9.5	49.7
H7 Neu5Ac	0.48881	0.13858	0.06773	10.6	55.7
H4 Neu5Ac	0.85632	0.06473	0.05542	8.7	45.5
H6 Neu5Ac	0.38828	0.16066	0.06238	9.8	51.3
H6 Gal	0.16369	0.31134	0.05096	8.0	41.9
H5 Gal	0.08258	0.66815	0.05517	8.7	45.3
H4 Gal	0.19587	0.3283	0.06430	10.1	52.8
H3 Gal	0.15749	0.29458	0.04639	7.3	38.1
NHAc Neu5Ac	0.49253	0.21648	0.10662	16.7	87.6
$H3_{eq}$ Neu5Ac	0.2296	0.2076	0.0476	7.5	39.2
NHAc GlcNAc	0.10359	0.5285	0.05474	8.6	44.9

Table S5. Interactions between ^{NSA}Neu5Ac and Siglec-8. S= salt bridge; H= hydrogen bond.

Contact type	Siglec-8 (monomer A) residue	BSA (Å²)
H	Y23	74
	Y27	12
	R72	22
	P73	16
H	Y74	40
	Q75	6
S	R125	20
	S130	4
	M131	5
	K132	39
	W133	31
H	S134	20
	K136	21
H	Q138	65
	L139	18
	N140	2
	Y141	10
	Total	**405**

Contact type	Siglec-8 (monomer B) residue	BSA (Å²)
	Y23	80
	Y27	8
	R72	23
	P73	10
	Y74	52
	Q75	5
	R125	16
	M131	9
	K132	35
	W133	30
	S134	20
	K136	20
	Q138	37
	L139	21
	Y141	12
	Total	**378**

SI References

(1) Schrödinger, L. The PyMol Molecular Graphics System, Versión 1.8. *Thomas Hold* **2015**. DOI: doi.org/10.1007/s13398-014-0173-7.2.